Int. J. Heat Mass Transfer. Vol. 36, No. 18, pp. 4299–4305, 1993
Printed in Great Britain

0017-9310/93 $6.00+0.00

The formation of negative- and positive-segregated bands during solidification of aluminum–copper alloys

Q. Z. DIAO and H. L. TSAI
Department of Mechanical and Aerospace Engineering and Engineering Mechanics,
University of Missouri-Rolla, Rolla, MO 65401, U.S.A.

(*Received* 5 *January* 1993 *and in final form* 17 *June* 1993)

Abstract—The evolution of macrosegregation, appearing in the form of negative- and positive-segregated bands, in an aluminum–copper alloy unidirectionally solidified from the bottom has been analyzed numerically. It is found that a negative-segregated band is formed in the solidified casting if the casting is quenched during solidification. On the other hand, a positive-segregated band is created resulting from a sudden decrease of heat extraction rate at the bottom of the casting. Multiple negative- and positive-segregated bands could be formed in the solidified casting if the thermal boundary condition at the bottom of the casting fluctuates with time. The predicted banding segregation in the solidified alloy compares favorably with the available experimental data.

INTRODUCTION

MACROSEGREGATION refers to a large scale non-uniformity of the local average composition over a long range in a solidified casting or ingot. Significant positive and/or negative segregation (i.e. solute concentration is higher or lower than the initial melt concentration) can be frequently found in a machined ingot. It has been reported that the formation of macrosegregation is related to the flow of solute-rich or poor liquid in the mushy zone (interdendritic fluid flow) and/or the floating or settling of equiaxed grains or detached dendrites during alloy solidification [1]. The fluid flow can be induced by solidification contraction and/or forced convection (e.g. in centrifugal casting) and/or surface tension (i.e. Marangoni effect), and/or natural convection caused by temperature and/or solute gradients. Different types of macrosegregation have been found, including inverse segregation, banding segregation, centerline segregation, under-riser segregation, top-end segregation, ghost bands, freckles, channel segregation, and A- or V-segregation [1–7]. Banding segregation usually appears as band-like solute-poor or solute-rich regions in a solidified ingot.

In the past, many experimental studies on the formation of macrosegregation have been reported (e.g. refs. [2–7]). McDonald and Hunt [2] concluded from their experimental work with the NH_4Cl–H_2O system that conditions favoring the formation of A-segregation include alloy elements with large density differences, a wide range of freezing temperature, a tall ingot producing large differences in hydrostatic head, and long freezing times. Generally, these conditions can enhance the interdendritic convection leading to the formation of macrosegregation. Streat and Weinberg [3] studied the formation of macrosegregation in tin–lead alloys resulting from density differences in the liquid. Using a new quenching technique in 1978, Fredriksson and Nilsson [4] were able to identify three types of macrosegregation phenomena caused by interdendritic convection in tin–lead alloys. Jackson [5] explained the mechanisms leading to the formation of ghost bands observed experimentally in steel castings. Fisher and Hunt [6] investigated the time required for gravitational interdendritic fluid flow to produce appreciable macrosegregation. They concluded that for Al–5.6% Cu alloys to avoid the formation of macrosegregation, the ingot has to be small enough to be completely mushy within 2 min and fully solidified within 15 min. Bridge and Beech [7] employed an X-ray sensitive TV camera to continuously monitor the solidification process of a small sample of Al–20.7% Cu alloy, and they observed directly the formation of channel segregation. Morgan *et al.* [8] studied the effect of ingot height to cross-section ratio and ingot taper on the formation of top-end segregation in steel ingots. It can be concluded that extensive experiments have been conducted and the mechanisms leading to the formation of macrosegregation are now well understood.

In contrast, the development of macrosegregation models is somewhat lagging behind, and can be generally divided into two stages. In the early stage, roughly before 1986, the modeling was limited to one-dimensional solidification, and/or the governing differential equations were not completely coupled. Hence, the modeling of macrosegregation was conducted only for simple conditions, such as the directional solidification processes. During the first stage, perhaps the most important contribution to the macrosegregation modeling was made by Flemings and co-workers [9–11]. Flemings and Nereo [9] developed the well-known 'local solute redistribution equation' to predict the formation of macrosegregation in castings resulting from the flow of solute-rich liquid to feed solidification contractions. The equation requires the temperature gradients, rate of temperature change, and fluid flow in the solidifying casting, which must be obtained independently by experiments or by assumptions. In spite of these limitations, Flemings *et al.* [10] employed the local solute redistribution equation to successfully predict the formation of inverse segregation, banding segregation, and segregation due to the change of cross-section area, which was verified by the experimental data obtained by Flemings and Nereo [11]. In their studies, the formation of positive or negative banding segregation was caused by a sudden change in cooling conditions during alloy solidification.

In the second stage, the 'continuum-type formulation' [12, 13] was established; and the solution of multi-dimensional coupled continuity, momentum, energy, and species equations became available. Employing the continuum formulation, Beckermann and Viskanta [13] were able to predict some of the double-diffusive phenomena observed in the experiments. However, their numerical calculations showed a considerable disagreement with the measurements. Bennon and Incropera [14] employed a similar continuum model to successfully predict the formation of channel type A-segregation. Neilson and Incropera [15, 16] studied the unidirectional solidification of aqueous NH_4Cl and the effects of induced fluid motion. They were able to predict the formation of freckles resulting from an unstable solutal gradient. However, in the above-mentioned continuum formulation, except for the buoyancy terms, a constant density was assumed throughout the entire casting and, as a result, the shrinkage effect was neglected.

Generally, there are two categories of alloys which could lead to the formation of macrosegregation. The first category corresponds to the alloys, such as steel–carbon alloys, in which the lighter carbon species is rejected during solidification. This will induce an unstable solutal gradient for a unidirectional solidification cooled from the bottom. Due to transparent, low operation temperatures, and its dendritic morphology, aqueous NH_4Cl has been frequently used in experimental or theoretical work to simulate a steel–carbon alloy (e.g. refs. [2, 14–16]). On the other hand, there is an important category of alloys, such as aluminum–copper alloys, in which the heavier copper species is rejected during solidification, creating a stable solutal gradient in unidirectional solidification cooled from the bottom (e.g. refs. [9–11]). As the solute-induced convection can enhance or suppress the temperature caused convection and subsequently the fluid flow in the solidifying alloy, the selection of alloys in experiment or modeling can result in different types of macrosegregation.

In the present study, the formation of banding segregation for a unidirectional solidification of aluminum–copper alloys cooled from the bottom will be presented. As discussed previously, for unidirectional solidification of aluminum–copper alloys cooled from the bottom, both stable temperature and concentration gradients are created, and the fluid flow is caused only by solidification contraction. Hence, in addition to the availability of experimental data, this provides the simplest situation, and serves as the first step to study the effect of fluid flow and other solidification parameters on the formation of banding segregation. The continuum formulation improved previously by Chiang and Tsai [17, 18] to include the shrinkage effects, has been extended recently by Chen and Tsai [19], and Diao and Tsai [20] to predict the formation of inverse segregation and to study the solute redistribution in the mushy zone for unidirectional solidification of aluminum–copper alloys cooled from the bottom. This model will be used in the present study.

MATHEMATICAL MODEL

For two-dimensional alloy solidification, the continuum formulation including the shrinkage effect developed previously [19, 20] is employed in the present study. The coupled continuity, momentum, energy, and species equations, subjecting to the required boundary conditions, were solved by an implicit control-volume-based finite difference procedure using the SIMPLEC algorithm. The domain change due to solidification shrinkage was handled by the front tracking method. In the modeling the desired casting cooling rate can be easily achieved by changing the effective heat transfer coefficient between the chill and the casting. Detailed discussion about the numerical method and the check of numerical accuracy were given in the previous papers [17, 18], and they will not be repeated here. Figure 1 shows the grid system used in the computation. The calculations were executed on Apollo DN10000 workstations. Typical CPU time for the calculation of each case is about 120 h.

RESULTS AND DISCUSSION

As shown in Fig. 1, a unidirectional solidification can be induced by passing some coolant at a desired temperature, T_c, through a chill plate placed at the bottom of the casting, while the other sides of the casting are insulated. Heat transfer between the chill plate and the casting is accomplished via an effective heat transfer coefficient (HTC) h_c. An Al–4.1% Cu alloy is used in the present study, and its thermophysical properties as well as the casting conditions are summarized in Table 1.

As the casting will start to solidify from the bottom, there will be an upward positive temperature gradient in the casting. Hence, it is expected that a stable temperature field exists in the casting and no natural convection due to inverse temperature gradients is

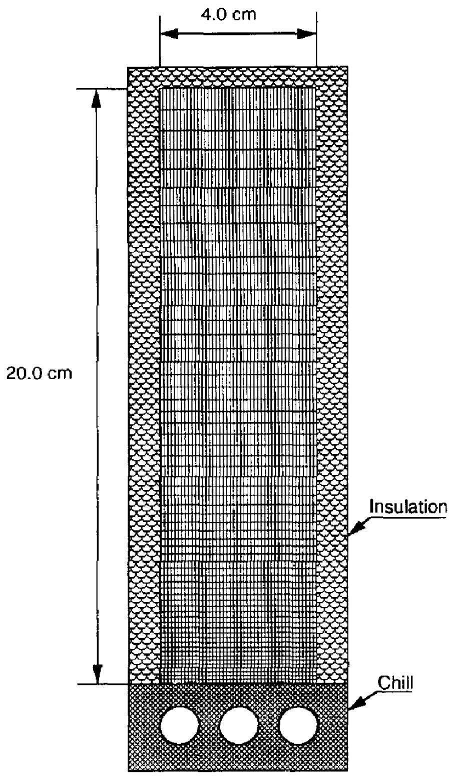

FIG. 1. Schematic representation of the physical domain and the grid system.

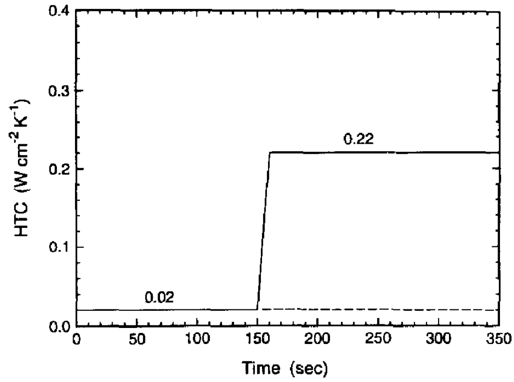

FIG. 2. Variation of effective heat transfer coefficient (HTC) between the chill and the casting as a function of time; HTC increases from 0.02 W cm^{-2} K^{-1} at time t = 150 s to 0.22 W cm^{-2} K^{-1} in 10 s, and remains constant thereafter.

present. Also, during alloy solidification, heavier copper species will be rejected starting from the bottom, creating a stable negative solutal gradient. In other words, neither the temperature gradients nor the concentration gradients will induce natural convection in the casting and, if solidification shrinkage is neglected, the casting is essentially uniform in composition since practical freezing rates preclude appreciable species diffusion [16]. Detailed results regarding the temperature, concentration, and velocity distributions in the casting during unidirectional solidification cooled from the bottom have been reported in the previous papers [19, 20], and they will not be repeated here.

The major objective in the present study is to investigate the formation of banding segregation when the thermal conditions at the bottom of the solidifying casting is suddenly changed. This can be easily achieved by rapidly increasing or decreasing the effective heat transfer coefficient between the chill and the casting. As the isoconcentrations of copper are planar in the horizontal direction, as discussed in refs. [19, 20], in the following only the distribution of solute concentration along the vertical direction of the casting will be given.

Figure 2 shows the time dependent effective heat transfer coefficient (HTC) between the chill and the casting. At time t = 150 s, HTC starts to increase from 0.02 to 0.22 W cm^{-2} K^{-1} in a period of 10 s, and then remains constant thereafter. For comparison, the case with constant HTC of 0.02 W cm^{-2} K^{-1} is also shown

Table 1. Thermophysical properties of Al–4.1% Cu and casting conditions, ref. [21] unless otherwise noted, * assumed

c_s	Solid specific heat (J g^{-1} K^{-1})	1.0928
c_l	Liquid specific heat (J g^{-1} K^{-1})	1.0588
D_s	Solid solute diffusion coefficient (cm^2 s^{-1})	≈ 0*
D_l	Liquid solute diffusion coefficient (cm^2 s^{-1})	3×10^{-5}*
k_s	Solid thermal conductivity (W cm^{-1} K^{-1})	1.9249
k_l	Liquid thermal conductivity (W cm^{-1} K^{-1})	0.8261
k_p	Equilibrium partition ratio	0.170
ρ_s	Solid density (g cm^{-3})	2.65
ρ_l	Liquid density (g cm^{-3})	2.40
β_T	Thermal expansion coefficient (K^{-1})	4.95×10^{-5}*
β_s	Solutal expansion coefficient	−2.0*
μ	Dynamic viscosity (g cm^{-1} s^{-1})	0.03
H	Latent heat (J g^{-1})	397.5
T_e	Eutectic temperature (K)	821.2
T_m	Fusion temperature (K)	933.2
$f^{\alpha}_{l,0}$	Initial copper concentration (Pct)	4.1
T_0	Initial alloy temperature (K)	970.0
T_c	Chill temperature (K)	293.0

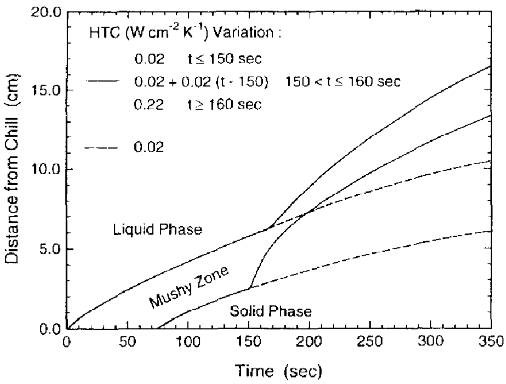

FIG. 3. Locations of the liquidus and solidus fronts, and the sizes of liquid phase, mushy zone, and solid phase, corresponding to the cooling conditions in Fig. 2.

in the figure. Corresponding to the cooling conditions in Fig. 2, Fig. 3 shows the locations of the liquidus front and solidus front in the casting, as well as the sizes of solid phase, mushy zone, and liquid phase, as a function of time. The size of the mushy zone increases with time until the solid phase is formed at about 75 s. The solidus front and liquidus front are almost parallel between 75 s and 150 s, indicating the solidification process is nearly a quasi-steady-state during this period, and almost an equal size of mushy zone is formed. The solidus front responds rapidly to the change of HTC at 150 s and moves upward due to a higher solidification rate. However, the liquidus front responds to the change of HTC about 20 s late, resulting in a significant decrease in the size of the mushy zone. The size of the mushy zone decreases to the minimum value at about 175 s, and then increases gradually thereafter. The dashed curves represent the case if the HTC remains constant, showing a slow but continuous increase in the size of the mushy zone.

Figure 4 illustrates a sequence of solute redistributions in the casting at different times, corresponding to the change of HTC given in Fig. 2. Except for the first solute distribution curve, each curve in the figure has three segments starting from the bottom of the casting, and each segment corresponds to the solid phase, mushy zone, and liquid phase, respectively. A positive-segregated (i.e. above the initial solute concentration) region near the bottom of the casting (called inverse segregation) is formed, which is accompanied by a moving negative-segregated (i.e. below the initial solute concentration) mushy zone. It is noted that, except near the solidus front (e.g. curve 2), the solute concentration in the mushy zone is below the initial value. The formation of inverse segregation near the bottom of the casting was analyzed in the previous paper [19], and will not be repeated here. The solute distribution at 170 s, which is 20 s after the HTC is increased at the bottom, shows a significant decrease in the size of the mushy zone and a more severe negative segregation. The minimum solute concentration in the mushy zone occurs when the size of the mushy zone reaches the minimum. Because the solidification rate is suddenly increased, there is not enough time for the solute to migrate, hence, the solute in the mushy zone is 'frozen', creating an embryo of a negative-segregated band in the solidified region.

At time $t = 180$ s, the original mushy zone has evolved two 'bands', one is in the solidified region, which is a 'stationary band'; and the other is a 'moving band' corresponding to the moving mushy zone. The moving mushy band is similar to, but smaller than, the original one (i.e. right before the quench was imposed). The formation of stationary and moving bands becomes more clear at time $t = 190$ s. It is noted that the solute distribution in the solid phase remains unchanged with time, because the solute diffusion in the solid phase is negligibly small. The moving band continues to move upward and its size increases gradually with time. Also, the solute concentration in the casting between the stationary band and the moving band is nearly uniform, but is slightly higher than the initial solute concentration. The trapezoidal rule was used to calculate the total areas with concentrations higher and lower than the initial value (i.e. 4.1% of copper) at time $t = 270$ s, and they are found nearly identical, indicating the overall solute is conserved. It is noted that the formation of negative banding segregation, shown by Fig. 4, has been predicted by Flemings *et al.* [10] using the local solute redistribution equation and the assumed liquidus and eutectic isotherm movement. They argued that the decrease in the size of the mushy zone, due to the change of solidification conditions, will result in the formation of negative banding segregation, which is consistent with the results predicted by the present model.

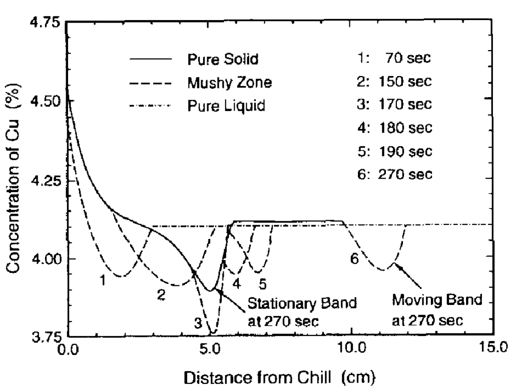

FIG. 4. Predicted distributions of solute concentration at different times, corresponding to the cooling conditions shown by the solid line in Fig. 2; initial copper concentration =4.1%.

The effect of different cooling conditions, including the beginning quenching time, the quenching rate (i.e. HTC increases to the same value in different periods of time), and the degree of quenching (i.e. HTC

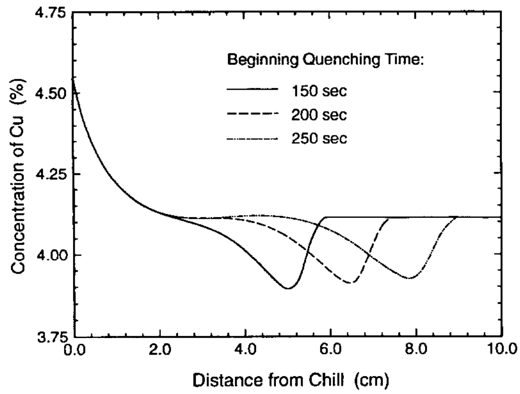

FIG. 5. Effect of the beginning quenching time on the formation of banding segregation; HTC increases from 0.02 W cm^{-2} K^{-1} at time t = 150 s, 200 s or 250 s, to 0.22 W cm^{-2} K^{-1} in 10 s, and remains constant thereafter.

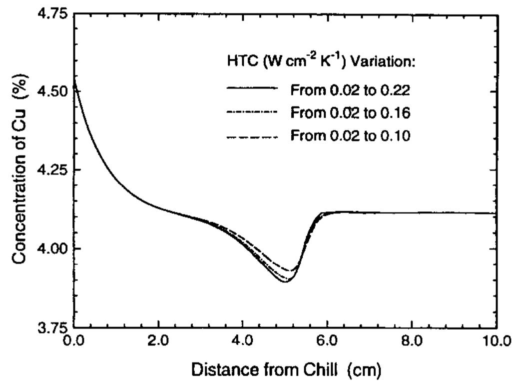

FIG. 7. Effect of the degree of quenching on the formation of banding segregation; HTC increases from 0.02 W cm^{-2} K^{-1} at time t = 150 s to 0.22 W cm^{-2} K^{-1}, 0.16 W cm^{-2} K^{-1}, or 0.10 W cm^{-2} K^{-1} in 10 s, and remains constant thereafter.

increases to different values in the same period of time) on the formation of banding segregation will be discussed next. Figure 5 shows the locations of the negative-segregated band in the solidified casting quenched at different times, while maintaining the same quenching rate and degree of quenching. The location of the banding segregation in the solidified casting is related to the location of the mushy zone when the quenching is imposed. Hence, the negative-segregated band is closer to the bottom of the casting when the casting is quenched at 150 s compared to those quenched later. A slightly severer segregated band is formed for the casting quenched earlier, because the mushy zone is closer to the bottom resulting in a stronger quenching power. Figure 6 shows the effect of quenching rate on the formation of banding segregation in the solidified casting. A higher quenching rate (i.e. shorter quenching period) results in a slightly greater negative segregation and the band shifts toward the bottom of the casting.

Figure 7 shows the banding segregation in the solidified region for three different degrees of quenching. It is seen that a stronger quenching at the bottom of the casting results in a severer negative segregation. This is consistent with the result discussed in Fig. 5. It is noted that in Figs. 5–7, a moving negative-segregated mushy band still exists at the location far away from the bottom of the casting, and is not shown in the figure. Figure 8 shows the existence of two negative-segregated bands in the solidified region and a moving mushy band, resulting from two quenches at the bottom of the casting. It is seen that the second stationary band is smaller and has less severe negative segregation than the first band. The solute distribution between any two bands is uniform and its value is greater than the initial solute concentration. The positive solute segregation near the bottom and in between the bands is compensated by the three negative-segregated bands, so that the overall conservation of solute is satisfied.

Figure 9 shows the evolution of solute redistribution when the heat extraction rate is suddenly decreased at the bottom of the casting, which is achieved by decreasing the heat transfer coefficient

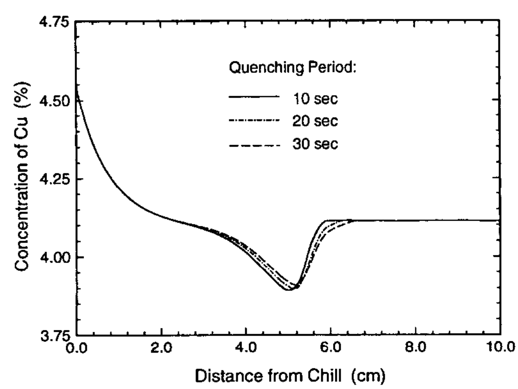

FIG. 6. Effect of the quenching rate on the formation of banding segregation; HTC increases from 0.02 W cm^{-2} K^{-1} at time t = 150 s to 0.22 W cm^{-2} K^{-1} in 10 s, 20 s, or 30 s, and remains constant thereafter.

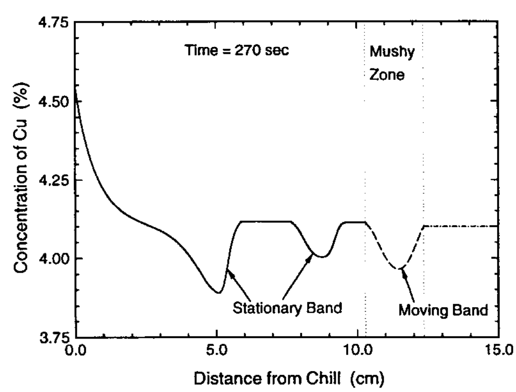

FIG. 8. The formation of two negative-segregated bands in the solidified casting; HTC increases from 0.02 W cm^{-2} K^{-1} at time t = 150 s to 0.22 W cm^{-2} K^{-1} in 10 s, remaining at 0.22 W cm^{-2} K^{-1} for 40 s, increasing to 1.62 W cm^{-2} K^{-1} in 5 s, and then remains constant thereafter.

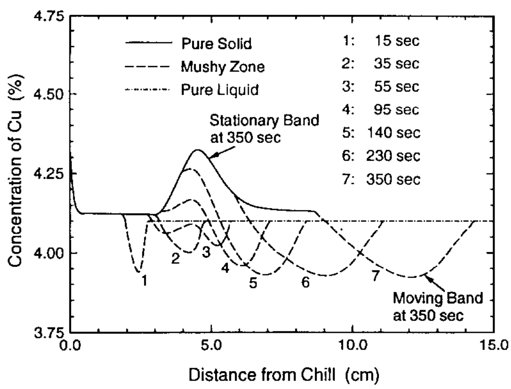

FIG. 9. The formation of positive-segregated band resulting from a decrease of heat extraction rate at the bottom of the casting; HTC decreases from 0.16 W cm^{-2} K^{-1} at time $t = 20$ s to 0.02 W cm^{-2} K^{-1} in 10 s, and remains constant thereafter.

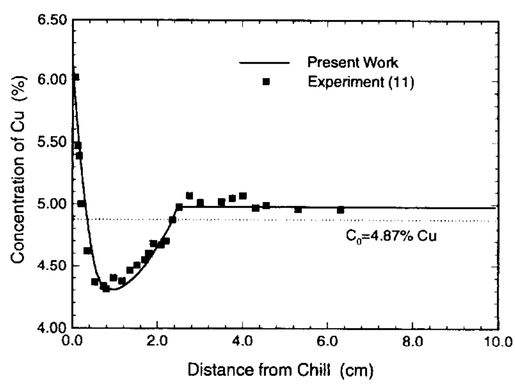

FIG. 10. Comparison of the predicted banding segregation and the experimental data.

between the casting and the chill. In an actual casting process, the decrease of heat transfer rate can be caused by the formation of a gap between the casting and the mold. For each curve in the figure, there are three segments each corresponding to the solid phase, mushy zone, and liquid phase. Comparing with Fig. 4, a greater heat extraction rate at the bottom of the casting causes a less severe inverse segregation, as discussed in ref. [20]. From curves 2 and 3 in Fig. 9, one can see that a remelting occurs near the solidus front shortly after the heat extraction rate is decreased. At time $t = 55$ s, curve 3, the solute distribution in the mushy zone appears like a W shape and a relative maximum solute concentration occurs near the center. This relative maximum solute concentration increases with time, and eventually forms a positive-segregated band in the solidified region. Hence, the original negative-segregated mushy zone gradually becomes a positive-segregated band in the solidified region, and an even larger moving negative-segregated mushy zone. The sudden decrease of solidification rate allows a longer time for more solute to pile up near the solidus front. This phenomenon is similar to the formation of inverse segregation near the bottom of the casting; showing a lower heat extraction rate creates a greater inverse segregation and a larger moving mushy zone, as discussed in ref. [20]. However, as the solidus front continues to move upward, the solute in the newly solidified region increases to a maximum value and then decreases to the 'normal' value, as shown by curve 7 in the figure. The formation of positive banding segregation has been predicted by Flemings *et al.* [10] using the local solute redistribution equation and the assumed liquidus and eutectic isotherm movement. They argued that the increase in the size of the mushy zone will lead to the formation of positive banding segregation, which is consistent with the present study.

From the above discussion, we can conclude that the formation of negative-segregated bands in the solidified casting is evolved from the moving negative-segregated mushy zone due to a sudden increase of solidification rate. The formation of positive-segregated bands is evolved from the moving negative-segregated mushy zone due to a sudden decrease of solidification rate. However, after the formation of either negative- or positive-segregated band, the moving negative-segregated mushy zone does not disappear, and it becomes either smaller or larger in the solidifying casting. It can be easily inferred that at least one additional negative-segregated band will eventually be formed in the casting at the location where the moving mushy zone is finally solidified. If the thermal boundary condition at the bottom of the casting fluctuates during solidification, several negative and positive segregation bands could be formed in the solidified casting.

Figure 10 shows one set of experimental data reported by Flemings and Nereo [11] for a unidirectional solidification of Al–4.87% Cu alloys, resulting from a sudden increase of the rate of heat extraction at the bottom. However, no detailed cooling conditions, such as the quenching rate and the beginning quenching time, were given in the paper. A numerical experiment was conducted using the present model, and the curve shown in Fig. 10 is the predicted banding segregation under the cooling conditions: HTC increases from 0.005 W cm^{-2} K^{-1} at time $t = 30$ s to 0.20 W cm^{-2} K^{-1} in a period of 10 s, and remains constant thereafter. It is seen that even with the available thermophysical properties for Al–4.1% Cu (Table 1), good agreement between the predicted results and the experimental data is obtained.

CONCLUSIONS

The evolution of banding segregation has been analyzed using the continuum formulation for a unidirectional solidification of Al–Cu alloys cooled from the bottom. Due to the flow of solute-rich liquid in the mushy zone caused by solidification contraction, a positive-segregated region is created near the bottom of the solidified casting (called inverse segregation), which is accompanied by a moving solute-poor mushy zone or band. When the solidifying casting is quenched at the bottom, the moving solute-poor mushy zone evolves two segregated bands, one is a stationary negative-segregated band in the solidified region, and the other is a moving solute-poor mushy band similar to, but smaller than, the original one. On the other hand, if the heat extraction rate at the bottom of the casting is suddenly decreased, the moving solute-poor mushy band becomes two segregated bands, one is a stationary positive-segregated band in the solidified region, and the other is a moving solute-poor mushy band similar to, but larger than, the original one. The location and severity of the banding segregation in the casting depend on the beginning quenching time, the quenching rate, and the degree of quenching. Multiple positive and negative bands could be formed in the casting if the cooling condition at the bottom of the casting fluctuates with time. The predicted banding segregation has been compared with the available experimental data, and good agreement was obtained.

Acknowledgement—This work was supported in part by the Air Force Office of Scientific Research under Contract No. F49620-88-C-0053/SB5881-0378, which is gratefully acknowledged.

REFERENCES

1. M. C. Flemings, *Solidification Processing*, pp. 214–258. McGraw-Hill, New York (1974).
2. R. J. McDonald and J. D. Hunt, Fluid motion through the partially solid regions of a casting and its importance in understanding A type segregation, *Trans. Metall. Soc. AIME* **245,** 1993–1997 (1969).
3. N. Streat and F. Weinberg, Macrosegregation during solidification resulting from density differences in the liquid, *Metall. Trans.* **5,** 2539–2548 (1974).
4. H. Fredriksson and S. O. Nilsson, On the formation of macrosegregations in ingots, *Metall. Trans.* **9B,** 111–120 (1978).
5. W. J. Jackson, Ghost bands in steel castings. In *Solidification Technology in the Foundry and Casthouse*, pp. 426–431. The Metal Society, London (1983).
6. K. M. Fisher and J. D. Hunt, Investigation of time required for gravitational interdendritic fluid flow mechanism to produce appreciable macrosegregation. In *Solidification Technology in the Foundry and Casthouse*, pp. 176–181. The Metal Society, London (1983).
7. M. R. Bridge and J. Beech, Formation of macrosegregation in large, as-cast masses: direct observation of some aspects. In *Solidification Technology in the Foundry and Casthouse*, pp. 478–483. The Metal Society, London (1983).
8. P. C. Morgan, P. W. Waterworth and I. G. Davies, Macrosegregation in killed steel ingots. In *Solidification Technology in the Foundry and Casthouse*, pp. 450–460. The Metal Society, London (1983).
9. M. C. Flemings and G. E. Nereo, Macrosegregation: part I, *Trans. Metall. Soc. AIME* **239,** 1449–1461 (1967).
10. M. C. Flemings, R. Mehrabian and G. E. Nereo, Macrosegregation: part II, *Trans. Metall. Soc. AIME* **242,** 41–49 (1968).
11. M. C. Flemings and G. E. Nereo, Macrosegregation: part III, *Trans. Metall. Soc. AIME* **242,** 50–55 (1968).
12. W. D. Bennon and F. P. Incropera, A continuum model for momentum, heat and species transport in binary solid–liquid phase change systems—I. Model formulation, *Int. J. Heat Mass Transfer* **30,** 2161–2170 (1987).
13. C. Beckermann and R. Viskanta, Double-diffusion convection during dendritic solidification of a binary mixture, *PCH PhysicoChemical Hydrodynamics* **10,** 195–213 (1988).
14. W. D. Bennon and F. P. Incropera, The evolution of macrosegregation in statically cast binary ingots, *Metall. Trans.* **18B,** 611–616 (1987).
15. D. G. Neilson and F. P. Incropera, Unidirectional solidification of a binary alloy and the effects of induced fluid motion, *Int. J. Heat Mass Transfer* **34,** 1717–1732 (1991).
16. D. G. Neilson and F. P. Incropera, Numerical study of the effects of transport phenomena on macrosegregation during unidirectional solidification of a binary substance, *Wärme- und Stoffübertragung* **27,** 1–10 (1992).
17. K. C. Chiang and H. L. Tsai, Shrinkage-induced fluid flow and domain change in two-dimensional alloy solidification, *Int. J. Heat Mass Transfer* **35,** 1763–1770 (1992).
18. K. C. Chiang and H. L. Tsai, Interaction between shrinkage-induced fluid flow and natural convection during solidification, *Int. J. Heat Mass Transfer* **35,** 1771–1778 (1992).
19. J. H. Chen and H. L. Tsai, Inverse segregation for a unidirectional solidification of aluminum–copper alloys, *Int. J. Heat Mass Transfer* **36,** 3069–3075 (1993).
20. Q. Z. Diao and H. L. Tsai, Modeling of solute redistribution in the mushy zone during solidification of aluminum–copper alloys, *Metall. Trans.* **24A,** 963–973 (1993).
21. R. D. Pehlke, A. Jeyarajan and H. Wada, Summary of thermal properties for casting alloys and mold materials, Report No. PB83-211003, National Technical Information Service, Washington, D.C. (1983).